Restricted Model Control applied to the Quanser Aero with uncertain parameters

Amélie Carrierou*, Cédric Join †, Jean-Philippe Condomines ‡
∗ and † are with CRAN, Université de Lorraine, BP 239, 54506 Vandœuvre-lès-Nancy, France
‡ is with ENAC, Université de Toulouse, 31400 Toulouse, France

ABSTRACT

This work study the impact on a Model-Free Control (MFC) feedback combined with flatness-based control, also know as Restricted-Model Control (RMC), in order to address the problem of robustness to uncertain parameters. The proposed control architecture, is applied to the half-quad Quanser Aero benchmark in two degree-of-freedom configuration. Tests focuse on the robustness of RMC to over-efficient propellers, under-efficient propellers and augmented friction.

1 INTRODUCTION

The number and diversity of applications involving Micro Air Vehicles (MAVs) are extensive and have received considerable attention in recent years. Among possible structures, quadrotor UAVs are a popular option for tasks that require highly agile maneuvers in complex, constrained environments. The Quanser laboratory-based two degree-of-freedom (2-DoF) helicopter system is an ideal platform for such studies due to its versatile design, which allows for the emulation of various flight dynamics and control scenarios. Its ability to operate in both single degree-of-freedom and two degree-of-freedom configurations makes it particularly useful for testing advanced control strategies under different dynamic conditions. Several advanced control techniques like optimal linear control ([1]), sliding mode ([2] and [3]) and adaptive control ([4]) have been employed. However, these approaches require the development of an accurate model describing the dynamics, which is costly and time-consuming.

Flatness-based control (see [5]) offers significant advantages due to its capacity to explicitly derive control inputs from desired trajectories. This approach ensures that complex trajectory planning and execution can be achieved with high accuracy, which is essential for MAVs operating in dynamic and constrained environments. However, real-world applications often involve uncertainties and unmodeled dynamics that can degrade the performance of model-based controllers. For this purpose, Model-Free Control (MFC, see [6]) theory, coupled with flatness-based control, has been developed, providing robustness and enhancing the performance of the control system.

The Quanser Aero, with its configurable propellers and adjustable friction settings, allows for a controlled environment to study the interplay between these two control strategies. By examining the effects of MFC feedback on a flatness-based control scheme, we can better understand how to mitigate the limitations of model-based control in the presence of real-world uncertainties. The experiments conducted on the Quanser Aero will provide valuable insights into the practical implementation of this combined control strategy, ultimately contributing to the development of more reliable and efficient control systems for MAVs.

While recalling the basic motion equations of the Quanser Aero in §II, the main contributions of this paper are therefore:

- to make explicit in §III the theoretical equations that describe RMC architecture in the benchmarking case of the Quanser Aero;
- to provide new preliminary results §IV, focusing on the behaviour of flatness-based control and Restricted-Model-Control with parameters variations.

2 SYSTEM DESCRIPTION

The Quanser Aero is a control benchmark proposed by the Canadian manufacturer Quanser [1]. It's a Multi-Input Muli-Output (MIMO) system with 2 configurations and a direct integration with Matlab-Simulink®. The Quanser Aero, represented Figure 1, have 2 propellers that can be rotated to be either horizontal or vertical. Thus this benchmark have two configurations. On the first one, both propellers are horizontal and this system have only one degree of freedom, pitch rotation. On the second one, one propeller is horizontal and the second one is vertical so this system have 2 degree of freedom, pitch and yaw rotation (see Figure 2). For this work we used the second configuration.

2.1 Modelling

As depicted in the free-body diagram in Figure 2, the horizontal propeller, controlled by the tension V_p, generates a force F_p and induces a torque τ_p, causing angular motion θ in the pitch plane (around the y axis). Similarly, the yaw rotor, driven by the tension V_y, produces an aerodynamic force

*Email address : amelie.carrierou@univ-lorraine.fr
†Email address : cedric.join@univ-lorraine.fr
‡Email address : jean-philippe.condomines@enac.fr

[1] https://www.quanser.com/products/quanser-aero/

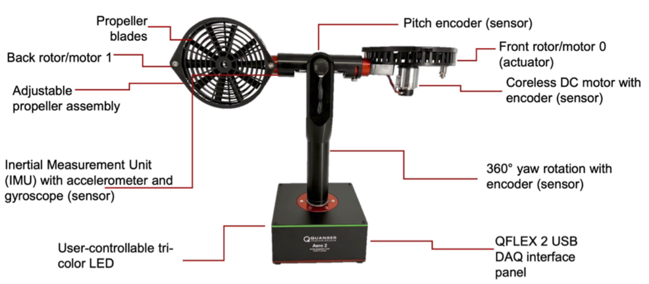

Figure 1: Quanser Aero : 2 degree of freedom configuration [image by Quanser Inc.]

F_y, resulting in torque τ_y and angular motion ψ in the yaw plane (around the z axis). These cross-torques cause significant cross-coupling between pitch and yaw channels. In the Quanser Aero documentation [7], a simple spring-mass-damper type of linear model that takes this coupling into account, is considered. The equations of motion are described in equation (1)

$$\begin{cases} J_p\ddot{\theta} + D_p\dot{\theta} + K_{sp}\theta = \tau_p \\ \\ J_y\ddot{\psi} + D_y\dot{\psi} = \tau_y \end{cases} \tag{1}$$

where τ_p and τ_y are related to their respective motor voltages by

$$\tau_p = K_{pp}V_p + K_{py}V_y, \quad \tau_y = K_{yp}V_p + K_{yy}V_y \tag{2}$$

From the point of view of state-space modelling, the state of this system is $\boldsymbol{x} = [\theta\ \psi\ \dot{\theta}\ \dot{\psi}]^T$, the input is $\boldsymbol{x} = [V_p\ V_y]^T$ and the output is $\boldsymbol{y} = [\theta\ \psi]^T$

Some of the parameters in equation (1) and equation (2) are given in the system's specification, while others were experimentally obtained. The values of the parameters are given by Table 1. In the above description, the term K_{sp} accounts for the gravitational force affecting the vertical motion (i.e, pitch), whereas no such factor is considered for the horizontal motion (i.e, yaw). It is important to note that in this model, the interaction between pitch and yaw movements is captured by the cross-terms K_{py} and K_{yp} with $|K_{py}| = |K_{pp}|$ and $|K_{yy}| = 1.5|K_{yp}|$ (see Table 1), the coupling from V_p to ψ is significantly more than the one from V_y to θ.

2.2 Settings

The Quanser Aero model allows for various modifications enabling versatile testing of control strategies and dynamic responses in different experimental scenarios. In this paper, we will concentrate on propeller configurations and friction settings. It is possible to modify the system in two ways to study different aerodynamic and control behaviors. Firstly, the system comes with two main configurations of propellers: a pair with 2 blades and another with 10 blades. Switching between these configurations allows observing how the propeller setup affects the generation of forces and moments, as well as the stability and maneuverability of the system. Secondly, the model offers the option to adjust friction on the horizontal axis by tightening or loosening a screw. This adjustment varies the perceived resistance and inertia by the system, thereby influencing its dynamic response and control accuracy.

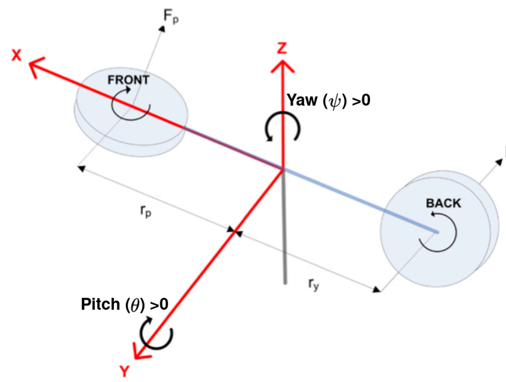

Figure 2: Free-body diagram of the Quanser Aero

Table 1: System parameters

Parameters (10 blades propeller)	Value/range
Moment of inertia about pitch axis ($\mathbf{Jp}$)	0.0219 kgm^2
Moment of inertia about yaw axis($\mathbf{J_y}$)	0.022 kgm^2
Damping about pitch axis ($\mathbf{D_p}$)	0.0113 Vs/rad
Damping about yaw axis ($\mathbf{D_y}$)	0.0131 Vs/rad
Stiffness about pitch axis ($\mathbf{K_{sp}}$)	0.0419 Nm/rad
Torque thrust gain from pitch rotor acting on pitch ($\mathbf{K_{pp}}$)	0.0013 Nm/V
Torque thrust gain from yaw rotor acting on yaw ($\mathbf{K_{yy}}$)	0.002 Nm/V
Torque thrust gain from yaw rotor acting on pitch ($\mathbf{K_{py}}$)	0.0016 Nm/V
Torque thrust gain from pitch rotor acting on yaw ($\mathbf{K_{yp}}$)	-0.0013 Nm/V

3 RESTRICTED MODEL CONTROL

Restricted Model Control (RMC, presented in [6] [8]) represents a compelling synthesis of two control methodologies : flatness-based and Model-Free Control (MFC).

Differential flatness was first introduced by M. Fliess and al. in [5]. It's a structural property of a system that can be used to compute nominal control input based on a dynamical model and a desired output. Flatness based control can successfully solve trajectory tracking problems for complex nonlinear systems like for example : induction drive [9], delay systems [10], partial differential equations [11], [12] and tilt-body UAV [13].

Model-Free Control term appears many times in the literature, but in distinct meanings from this paper. Actually, the growing importance of artificial intelligence and machine learning techniques, particularly through neural networks, has naturally been implanted into the model-free terms: see, for example [14] and [15]. However, in this paper, we assume Model-Free Control terms according to [16].

3.1 Flatness based controller

Consider a system with state $\boldsymbol{x}(t) \in \mathbb{R}^n$ and input $\boldsymbol{u}(t) \in \mathbb{R}^m$ defined by equation 3.

$$\dot{\boldsymbol{x}}(t) = f(\boldsymbol{x}(t), \boldsymbol{u}(t)) \tag{3}$$

This system is said deferentially flat, or just flat, if it exist $\boldsymbol{z}(t) \in \mathbb{R}^m$, called flat output, defined by equation (4) and two function A and B such as the state and the control input and be express based on this flat output.

$$\boldsymbol{z}(t) = \Phi(\boldsymbol{x}(t), \boldsymbol{u}(t), \dot{\boldsymbol{u}}(t), \cdots, \boldsymbol{u}^{(\phi)}(t)) \tag{4}$$

$$\boldsymbol{x}(t) = A(\boldsymbol{z}(t), \dot{\boldsymbol{z}}(t), \cdots, \boldsymbol{z}^{(\alpha)}(t)) \tag{5}$$

$$\boldsymbol{u}(t) = B(\boldsymbol{z}(t), \dot{\boldsymbol{z}}(t), \cdots, \boldsymbol{z}^{(\beta)}(t)) \tag{6}$$

For flatness-based control we need to have a smooth enough reference flat output trajectory $\boldsymbol{z}^*(t)$. Then we use this reference trajectory and equation (6) to compute the nominal input $\boldsymbol{u}^*(t)$. The global input, $\boldsymbol{u}(t)$ is the sum of the nominal input and a feedback term, $\boldsymbol{\delta u}(t)$

$$\boldsymbol{u}(t) = \boldsymbol{u}^*(t) + \boldsymbol{\delta u}(t) \tag{7}$$

Coming back to the Quanser Aero, the output of the system, $\boldsymbol{y}(t) = [\theta(t)\ \psi(t)]^T$ is a flat output. The state vector is trivially obtained with this flat output and its derivative. The relation between the flat output and the input vector is given by equation (8).

$$\begin{cases} V_p = \dfrac{J_p\ddot{\theta} + D_p\dot{\theta} + K_{sp}\theta}{K_{pp} - K_{py}K_{yp}K_{yy}^{-1}} - \dfrac{K_{yp}(J_y\ddot{\psi} + D_y\dot{\psi})}{K_{pp}K_{yy} - K_{py}K_{yp}} \\ \\ V_y = \dfrac{J_y\ddot{\psi} + D_y\dot{\psi} - K_{yp}V_p}{K_{yy}} \end{cases} \tag{8}$$

With this equation and a twice derivable reference trajectory $[\theta^*(t)\ \psi^*(t)]^T$ we have the nominal control input, $[V_p^*(t)\ V_y^*(t)]^T$. The next step is to choose a feedback $[\delta V_p(t)\ \delta V_y(t)]^T$.

With a linear system, one of the simplest choice is to use a feedback proportional to the position error. For the Quanser Aero this gives :

$$V_p = V_p^* + \delta V_p \tag{9}$$

$$V_y = V_y^* + \delta V_y \tag{10}$$

with :

$$\delta V_p = K_1(\theta - \theta^*) + K_2(\psi - \psi^*) \tag{11}$$

$$\delta V_y = K_3(\theta - \theta^*) + K_4(\psi - \psi^*) \tag{12}$$

But it's also possible to construct more a interesting feedback using, for example a data-based control law.

3.2 Flatness-based model-free control

Model-Free Control (MFC) is a data-based control architecture proposed by M. Fliess, C. Join and H. Sira-Ramirez ([16]). This controller uses an ultra-local model, given by equation (13), to estimate the unknown dynamic of a system. In this model, ν is the derivative order of y (in general 1 or 2) and α a parameter representing the impact of the input on the dynamic of the output. Both ν and α are chosen by the practitioner. The key step of this theory is the estimation of $F(t)$. It can be made by considering $F(t)$ as a piecewise constant function and using the algebraic estimation technique proposed in [17].

$$y^{(\nu)}(t) = F(t) + \alpha u(t) \tag{13}$$

Once we have $\hat{F}(t)$, the estimate of $F(t)$, the control input is given by equation (14) with $C(e(t))$ a PID controller and $y^*(t)$ a reference output trajectory.

$$u(t) = \frac{-\hat{F}(t) + y^{*(\nu)}(t) + C(e(t))}{\alpha} \tag{14}$$

MFC can be used when there is limited information about the system or when the model is not precise enough. It can also complement model-based controllers to compensate for unmodeled system dynamics.

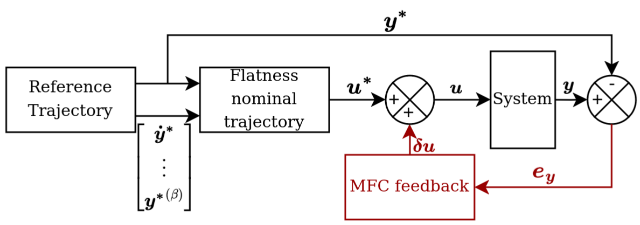

Figure 3: Restricted-Model Controller

The combination of flatness based control and MFC is called Restricted Model Control (RMC). A diagram of this control strategy is proposed figure 3, (to keep this diagram clear, we illustrated the case where the output of the system is also a flat output). In the RMC architecture, the ultra-local model given by equation (13) is adapted to represent the dynamic of the error $e_y = y - y^*$ thus we have :

$$e_y^{(\nu)}(t) = F(t) + \alpha\delta u(t) \tag{15}$$

From this model, equation (14) is rewrited stabilised the error in 0.

$$\delta u(t) = \frac{-\hat{F}(t) + C(e(t))}{\alpha} \tag{16}$$

For the Quanser Aero, the ultra-local model have to be adapted for a MIMO systems. Extension of MCF to this kind of systems where used in [18] and [19]. Since the cross coupling gains, K_{py} and K_{yp}, are important, we choose to use coupled ultra-local model. By taking the second derivative of the position errors, we have an ultra-local model given by :

$$\begin{cases} \ddot{e}_\theta(t) = F_\theta(t) + \alpha_{pp}\delta V_p(t) + \alpha_{py}\delta V_y(t) \\ \ddot{e}_\psi(t) = F_\psi(t) + \alpha_{yp}\delta V_p(t) + \alpha_{yy}\delta V_y(t) \end{cases} \tag{17}$$

Using the previously mentioned algebraic technique, an estimation of F_θ can be :

$$\hat{F}_\theta(t) = \frac{60}{T_{f\theta}^5}\int_0^{T_{f\theta}} \left((T_{f\theta}-\tau)^2 - 4\tau(T_{f\theta}-\tau) + \tau^2\right)\tilde{e}_\theta(\tau) - \frac{\alpha_{pp}}{2}\tau^2(T_{f\theta}-\tau)^2\delta\tilde{V}_p(\tau) - \frac{\alpha_{py}}{2}\tau^2(T_{f\theta}-\tau)^2\delta\tilde{V}_y(\tau)d\tau \tag{18}$$

with $T_{f\theta}$ the time window, $\tilde{e}_\theta(\tau) = e_\theta(\tau+t-T_{f\theta})$, $\delta\tilde{V}_p(\tau) = \delta V_p(\tau+t-T_{f\theta})$ et $\delta\tilde{V}_p(\tau) = \delta V_y(\tau+t-T_{f\theta})$. $\hat{F}_\psi$ is computed by replacing $T_{f\theta}$ by $T_{f\psi}$, $\tilde{e}_\theta(\tau)$ by $\tilde{e}_\psi(\tau)$, α_{pp} by α_{yp} and α_{py} by α_{yy} .

The quality of this estimation depend on the choice of $T_{f\theta}$. To have a good estimate, $T_{f\theta}$ have to bee small enough but a larger $T_{f\theta}$ guarantee better robustness to measurement noise.

With the two equations of the system (17) we can obtain the expression of $\delta V_y(t)$ given by equation (19). Then, with the first equation of this system, we have the expression for $\delta V_p(t)$ (equation (20)). Once we have those equations, we can use $\hat{F}_\theta(t)$ and $\hat{F}_\psi(t)$ to compute the values of $\delta V_y(t)$ and $\delta V_p(t)$.

$$\delta V_y(t) = \frac{-\hat{F}_\psi(t) + C(e_\psi(t))}{\alpha_{yy} - \alpha_{py}\alpha_{yp}\alpha_{pp}^{-1}} - \frac{\alpha_{yp}(\hat{F}_\theta - C(e_\theta(t))}{\alpha_{pp}\alpha_{yy} - \alpha_{py}\alpha_{yp}} \tag{19}$$

$$\delta V_p(t) = \frac{-\hat{F}_\theta(t) - \alpha_{py}\delta V_y + C(e_\theta(t))}{\alpha_{pp}} \tag{20}$$

For $C(e_\psi(t))$ and $C(e_\theta(t))$ we have chosen a proportional derivative controller :

$$C(e(t)) = k_p e(t) + k_d\dot{e}(t) \tag{21}$$

With a desired double pole s_d the k_p and k_d gains are :

$$k_p = -s_d^2 \tag{22}$$
$$k_d = -2s_d \tag{23}$$

Starting from a flatness-based controller, RMC require to chose a order of derivation, ν, the α parameter and the time window T_f used for estimation. Those parameters are adjusted based on trials and fails. The choice of α can be guided by the model and the choice of T_f depends on the dynamic of the systems and the measurement noise. Compared to the research of a flat input and the computation of nominal trajectory, the tuning of RMC parameters does not require a lot of effort but can improve the flatness-based control, especially in the case of partially know dynamics or imprecise model.

4 TESTS AND RESULTS

We now apply the control approach described in the previous section for Quanser Aero whose specifications are described in Table I. The idea is to investigate the impact of MFC feedback on flatness-based control in terms of uncertain parameters.

To investigate the impact of MFC feedback on flatness-based control, we leveraged the capability to modify the behavior of the Quanser Aero. The objective of the tests was to track a step signal in pitch while maintaining yaw at 0 degrees. Both control laws require the reference signal to be at least twice differentiable, thus the step signal was filtered by a discreet second-order system. The relation between θ_{ref} (the reference) and θ^* (filtered reference) and its first and second derivative are given by equation (24) to (26) with T_e the sampling time of the Quanser Aero.

$$\theta^*(t) = \frac{\theta_{ref}(t) + (2*\omega + 2*\omega^2)*\theta^*(t-T_e) - \omega^2*\theta^*(t_2T_e)}{\omega^2 + 2\omega + 1} \tag{24}$$

$$\dot{\theta}^*(t) = \frac{\theta_{ref}(t) - \theta^*(t-T_2)}{T_e} \tag{25}$$

$$\ddot{\theta}^*(t) = \frac{\theta_{ref}(t) - 2\theta^*(t-T_e) + \theta^*(t-2T_e)}{T_e^2} \tag{26}$$

The ω parameter is used to tune the filter. With $\omega = 300$ the input (θ_{ref}) and filtered input (θ^*) are presented figure 4.

to maximise the cases studied, the tests have been dived in two categories :

1. Tests with a 10 blades nominal system (Figures 5 to 8)
2. Tests with a 2 blades nominal system (Figures 9 to 12)

In both cases the nominal trajectory computation and controllers tuning where made on the nominal system then used without any modification on the altered system. One the first case (10 blades nominal system) we have studied the effect of an under-efficient propellers and augmented friction. On

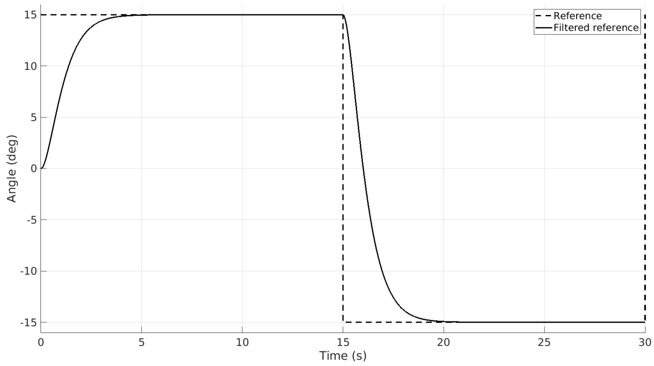

Figure 4: Reference and filtered reference

the second one, the effects of over-efficient propellers where tested.

The tuning of the two controllers for those both cases are presented table 2. Since the objectives and dynamics are different in pitch and yaw regulation thus two different sizes of time window are used. We have $T_{f\theta} = 0.1$s and $T_{f\psi} = 0.5$s. We also used the same α parameters for the two RMC controller : $\alpha_{pp} = 0.35$, $\alpha_{py} = 0.02$, $\alpha_{yp} = -0.02$ and $\alpha_{yy} = 1$.

Table 2: Values of gains tuning

Gains	10 blades system	2 blades system
K_1	-200	-480
K_2	90	80
K_3	-200	-480
K_4	-90	-80
s_θ	3	3.8
s_ψ	4.1	7.5

The gains presented in the table above where chosen to ensure the best pitch trajectory following while trying to maintain a reasonable disturbance rejection on yaw.

Since the feedback term for the flatness based controller is only proportional to positions errors, the steady state error in nominal cases was expected. Our objective is to study the impact of parameters variation on both control laws, not there trajectory tracking performances.

As shown in Figure 6 under-efficient propellers (yellow line) increased the steady state error compared to nominal case (red line). In the first 15 seconds the value of the error was increased by 13% and by 17% in the last 15 seconds. Restricted-Model Control (Figure 5) achieved to nullify this steady-state error, with nominal and under-efficient propellers, while preserving a good behaviour in transient response. This better response in pitch come at the prise of a poorer disturbance rejection in yaw (Figure 7 for RMC and 8 for flatness-based control).

With increased friction (green line), flatness-based control have the same kind of result with a more important effect on transient response but a lower steady-state error on the lasts 15 seconds (11%). Like on the previous test, the RMC converge at the same pitch value than on the nominal case, with some small oscillations on the transient response. To follow the pitch trajectory despite this modification, the RMC generate a higher control input, which leads to greater perturbation on yaw (with pics value of $+16$ degree and -13.5 degree for RMC, see Figure 5). The same effect is observed on flatness-based regulation but with much lower pics value.

Our last tests where made on with a 2 blades nominal system to tests the effect of over efficient propellers. Since the propeller is less effective, the reference amplitude for pitch was divided by two. With this lower amplitude, the coupling effect is less important so the yaw response is great for both controllers (error between -1 and 1 degree for RMC and -0.5 and 0.9 degree for flatness-based controller). For pitch trajectory following, the controller have better performances in transient and steady-state response. But on the flatness-based controller response, especially in figure 12, we can see some regular oscillations on the yellow curve. With higher feedback gains values those oscillations had lead to instability. We did not had this problem with RMC. With this lower reference output value we also had difficulties with the high quantization step size of the Quanser Aero.

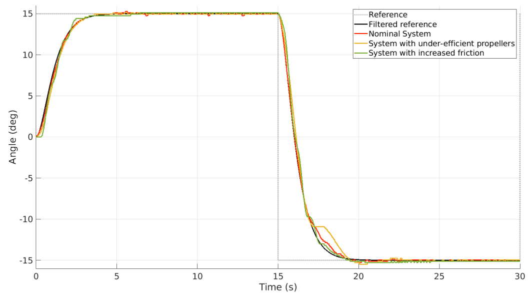

Figure 5: Pitch response, RMC, 10 blades nominal system

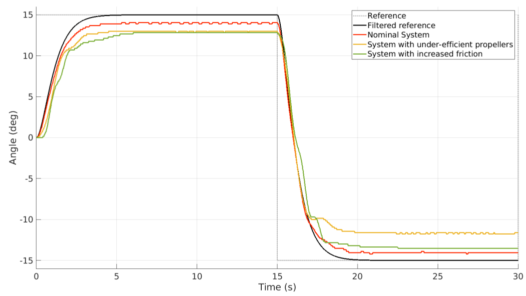

Figure 6: Pitch response, flatness controller, 10 blades nominal system

In all our tests, RMC has shown more robustness to parameters variation in the pitch response but at the price of a poorer yaw response. This is show that the MFC feedback

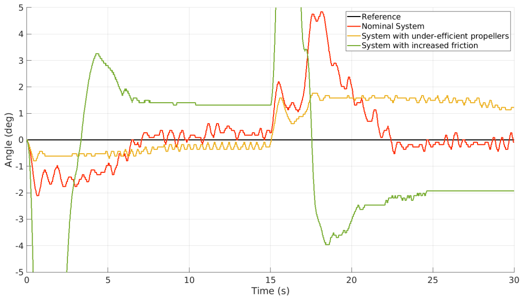

Figure 7: Yaw response, RMC, 10 blades nominal system

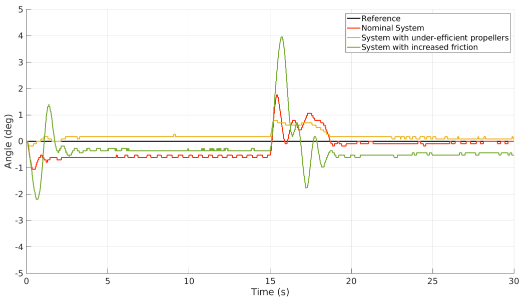

Figure 8: Yaw response, flatness controller, 10 blades nominal system

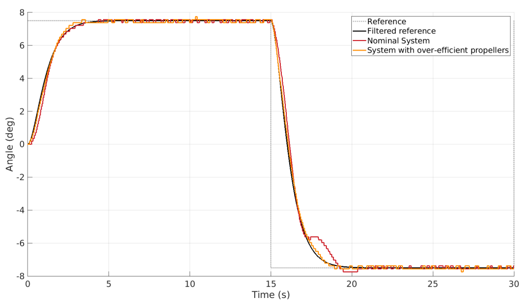

Figure 9: Pitch response, RMC, 2 blades nominal system

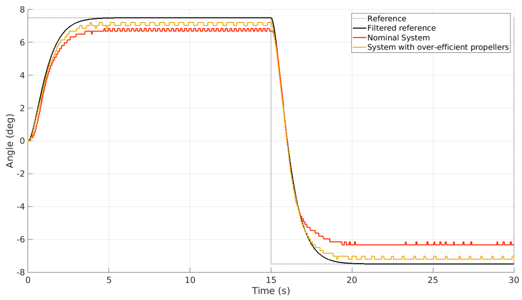

Figure 10: Pitch response, flatness controller, 2 blades nominal system

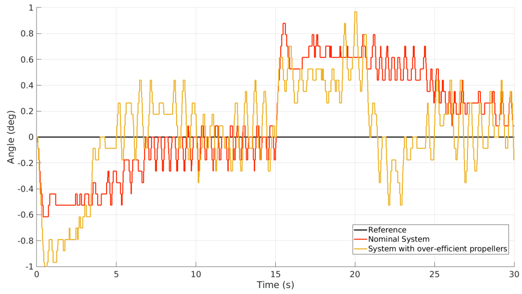

Figure 11: Yaw response, RMC, 2 blades nominal system

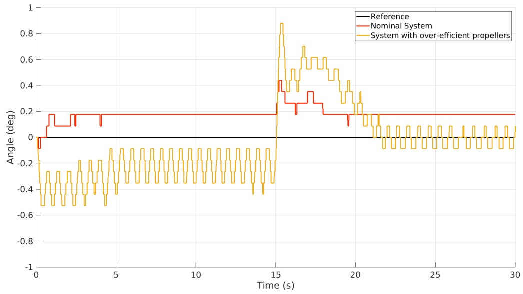

Figure 12: Yaw response, flatness controller, 2 blades nominal system

can improve a flatness based control law in when the model is partially known.

5 CONCLUSION

In this paper, we have design a MIMO Restricted-Model Controller for the 2 DoF Quanser Half-quad in order to address the problem of uncertain parameters identification. The proposed design was test on several cases and compared with flatness-based control. Those tests have shown that Model-Free Control can be used to improve the adaptive properties of flatness-based control.

This preliminary study has produced encouraging results and this control strategy will be applied on quadrotor MAV on future work.

REFERENCES

[1] Falguni Gopmandal and Arun Ghosh. Lqr-based mimo pid control of a 2-dof helicopter system with uncertain cross-coupled gain. *IFAC-PapersOnLine*, 55(22):183–188, 2022.

[2] Peter Lambert and Mahmut Reyhanoglu. Observer-based sliding mode control of a 2-dof helicopter system. In *IECON 2018-44th Annual Conference of the IEEE Industrial Electronics Society*, pages 2596–2600. IEEE, 2018.

[3] Sami Labdai, Larbi Chrifi-Alaoui, Saïd Drid, Laurent Delahoche, and Pascal Bussy. Real-time implementa-

tion of an optimized fractional sliding mode controller on the quanser-aero helicopter. In *2020 International Conference on Control, Automation and Diagnosis (ICCAD)*, pages 1–6. IEEE, 2020.

[4] Fouad Yacef, Nesrine Benkhaled, Lina Benhammouda, Lamia Melkou, Laid Degaa, Nassim Rizoug, and Mahmoud Belhocine. Adaptive intelligent control of 2-dof helicopter system. In *2023 9th International Conference on Control, Decision and Information Technologies (CoDIT)*, pages 2734–2739. IEEE, 2023.

[5] M Fliess, J Lévine, P Martin, and P Rouchon. On differentially flat nonlinear systems. *IFAC Proceedings Volumes*, 25(13):159–163, 1992.

[6] Michel Fliess and Cédric Join. Model-free control. *International journal of control*, 86(12):2228–2252, 2013.

[7] Quanser. Quanser aero 2 dof lab guide, 2016.

[8] Jorge Villagra and David Herrero-Pérez. A comparison of control techniques for robust docking maneuvers of an agv. *IEEE Transactions on Control Systems Technology*, 20(4):1116–1123, 2011.

[9] Veit Hagenmeyer and Emmanuel Delaleau. Continuous-time non-linear flatness-based predictive control: an exact feedforward linearisation setting with an induction drive example. *International Journal of Control*, 81(10):1645–1663, 2008.

[10] Maria Bekcheva, Hugues Mounier, and Luca Greco. Control of differentially flat linear delay systems with constraints. *IFAC-PapersOnLine*, 50(1):13348–13353, 2017.

[11] AF Lynch and J Rudolph. Flatness-based boundary control of a class of quasilinear parabolic distributed parameter systems. *International Journal of Control*, 75(15):1219–1230, 2002.

[12] Birgit Schörkhuber, Thomas Meurer, and Ansgar Jüngel. Flatness of semilinear parabolic pdes—a generalized cauchy–kowalevski approach. *IEEE Transactions on Automatic Control*, 58(9):2277–2291, 2013.

[13] Ezra Tal and Sertac Karaman. Accurate tracking of aggressive quadrotor trajectories using incremental nonlinear dynamic inversion and differential flatness. *IEEE Transactions on Control Systems Technology*, 29(3):1203–1218, 2020.

[14] Timothy P Lillicrap, Jonathan J Hunt, Alexander Pritzel, Nicolas Heess, Tom Erez, Yuval Tassa, David Silver, and Daan Wierstra. Continuous control with deep reinforcement learning. *arXiv preprint arXiv:1509.02971*, 2015.

[15] Mircea-Bogdan Radac, Radu-Emil Precup, and Raul-Cristian Roman. Model-free control performance improvement using virtual reference feedback tuning and reinforcement q-learning. *International Journal of Systems Science*, 48(5):1071–1083, 2017.

[16] Michel Fliess, Cédric Join, and Hebertt Sira-Ramirez. Complex continuous nonlinear systems: their black box identification and their control. *IFAC Proceedings Volumes*, 39(1):416–421, 2006.

[17] Michel Fliess and Hebertt Sira-Ramirez. An algebraic framework for linear identification. *ESAIM: Control, Optimisation and Calculus of Variations*, 9:151–168, 2003.

[18] Frédéric Lafont, Jean-François Balmat, Nathalie Pessel, and Michel Fliess. A model-free control strategy for an experimental greenhouse with an application to fault accommodation. *Computers and Electronics in Agriculture*, 110:139–149, 2015.

[19] Ouassim Bara, Michel Fliess, Cédric Join, Judy Day, and Seddik M Djouadi. Toward a model-free feedback control synthesis for treating acute inflammation. *Journal of theoretical biology*, 448:26–37, 2018.